Chemical Science International Journal

25(1): 1-9, 2018; Article no.CSIJ.45004
ISSN: 2456-706X
(Past name: American Chemical Science Journal, Past ISSN: 2249-0205)

Structural and Thermal Studies on Racemic $PbC_4H_4O_6•2H_2O$ Single Crystal

Takanori Fukami[1*] and Shuta Tahara[1]

[1]Department of Physics and Earth Sciences, Faculty of Science, University of the Ryukyus, Okinawa 903-0213, Japan.

Authors' contributions

This work was carried out in collaboration between both authors. Author TF performed the measurements and analyses and wrote the first draft of the manuscript. Author ST read, revised and approved the final manuscript.

Article Information

DOI: 10.9734/CSJI/2018/45004
Editor(s):
(1) Dr. Francisco Marquez-Linares, Department of Chemistry, Nanomaterials Research Group, School of Science and Technology, University of Turabo, USA.
Reviewers:
(1) Jaime Escalante, Universidad Autonoma del Estado de Morelos, Mexico.
(2) Renata Diniz, Universidade Federal de Minas Gerais, Brazil.
(3) Norhayati Hashim, Universiti Pendidikan Sultan Idris, Malaysia.
Complete Peer review History: http://www.sciencedomain.org/review-history/27566

Original Research Article

Received 20 September 2018
Accepted 23 November 2018
Published 04 December 2018

ABSTRACT

Single crystals of racemic lead tartrate dihydrate, $PbC_4H_4O_6·2H_2O$, were grown at 308 K by the gel method using silica gel as the growth medium. Differential scanning calorimetry, thermogravimetric-differential thermal analysis, and X-ray diffraction measurements were performed on the single crystals. The space group symmetry (orthorhombic *Pbca*) and the structural parameters were determined at room temperature. The structure consisted of PbO_8 polyhedra, $C_4H_4O_6$ molecules, two independent H_2O molecules, and zig-zag hydrogen-bonded chains along the *a*- and *b*-axes linked by O–H···O hydrogen bonds between adjacent molecules. Weight losses due to thermal decomposition of racemic $PbC_4H_4O_6·2H_2O$ occurred in the temperature range of 300–1600 K. We suggested that the weight losses in the ranges of 300–900 K and 900–1600 K were caused by the evolution of gases from $2H_2O$ and $C_4H_4O_5$, and the evaporation of PbO, respectively.

Keywords: Racemic $PbC_4H_4O_6•2H_2O$; crystal structure; thermal decomposition; TG-DTA; X-ray diffraction.

**Corresponding author: E-mail: fukami@sci.u-ryukyu.ac.jp;*

1. INTRODUCTION

Many tartrate compounds are formed by reacting tartaric acid (chemical formula: $C_4H_6O_6$; systematic name: 2,3-dihydroxybutanedioic acid) with compounds containing positive ions (two monovalent cations or one divalent cation) [1–6]. Tartaric acid has two chiral carbon atoms in its structure, which provides the possibility for four possible different forms of chiral, racemic, and achiral isomers: L(+)-tartaric, D(-)-tartaric, racemic (DL-) tartaric, and meso-tartaric acid [6–8]. Some of these compounds are of interest because of their physical properties, particularly their excellent dielectric, ferroelectric, piezoelectric, and nonlinear optical properties [1,9–11]. Moreover, they were formerly used in numerous industrial applications, for example, as transducers and in linear and non-linear mechanical devices [1,4,11].

Ridder et al. reported the crystal structure of lead L-tartrate, L-$PbC_4H_4O_6$, with space group $P2_12_12_1$, determined at room temperature by means of powder X-ray diffraction [12]. Weil later reported its accurate structure, confirmed by a single-crystal X-ray diffraction study, and the structural features were identified as follows [13]. Each Pb atom is bonded to eight O atoms of five $C_4H_4O_6$ molecules, while the tartrate molecule is linked to four Pb atoms. Further, the Pb atom has a coordination number of eight bonds with a cut-off value of about 3 Å for the ligating O atoms. The three-dimensional framework is stabilised by O–H···O hydrogen bonds between the O–H groups of the $C_4H_4O_6$ molecule and carboxylate O atoms of adjacent molecules.

Recently, we determined the crystal structure of racemic barium tartrate monohydrate, DL-$BaC_4H_4O_6{\cdot}H_2O$, by means of single-crystal X-ray diffraction [14]. The crystal structure was monoclinic with space group $P2_1/c$, and consisted of BaO_9 and BaO_{10} polyhedra, $C_4H_4O_6$ and H_2O molecules, and hydrogen-bonded chains extending in the *bc*-plane by O–H···O hydrogen bonds between adjacent molecules. Moreover, the chemical reactions occurring during thermal decomposition of DL-$BaC_4H_4O_6{\cdot}H_2O$ were found in the temperature range of 300–1550 K. Weight losses due to the thermal decomposition were caused by the evolution of H_2O, $2H_2CO$, 5CO, and $2O_2$ gases, and the resulting white and black substances in the vessel after decomposition were barium oxide (BaO) and barium monocarbide (BaC), respectively.

As mentioned above, it is expected that a racemic lead tartrate crystal can be synthesised using Pb^{2+} ions as divalent cations and DL-tartaric acid. In this paper, we report the synthesis of single crystals of racemic lead tartrate dihydrate, DL-$PbC_4H_4O_6{\cdot}2H_2O$, using the gel method, and determine their crystal structures at room temperature using X-ray diffraction. Moreover, the thermal properties of the lead crystal are studied by means of differential scanning calorimetry (DSC) and thermogravimetric-differential thermal analysis (TG-DTA).

2. EXPERIMENTAL

2.1 Crystal Growth

Single crystals of DL-$PbC_4H_4O_6{\cdot}2H_2O$ were grown in a silica gel medium at 308 K using the single test tube diffusion method. The gels were prepared in test tubes (length of 200 mm, and diameter of 30 mm) using aqueous solutions of Na_2SiO_3 (25 ml of 1 M), DL-$C_4H_6O_6$ (25 ml of 1 M), and CH_3COOH (25 ml of 1 M), and aged for six days. A solution of $Pb(NO_3)_2$ (30 ml of 0.5 M) was then gently poured on top of the gel, and the test tubes containing the gel and solution were placed in a drying apparatus kept at the constant temperature of 308 K by a temperature control unit. The crystals shown in Fig. 1 were harvested after six months. Small crystal seeds nucleated at the gel-solution interface and grew in the direction of gravity in the gel medium. Samples used for measurements were cut from transparent areas on the growing tips of the crystals.

2.2 Structure Determination

The X-ray diffraction measurements were carried out using a Rigaku Saturn CCD X-ray diffractometer with graphite-monochromated Mo K_α radiation (λ = 0.71073 Å). The diffraction data were collected at 299 K using an ω scan mode with a crystal-to-detector distance of 40 mm, and processed using the CrystalClear software package. The intensity data were corrected for Lorentz polarisation and absorption effects. The structures were solved by direct methods using the SIR2011 program and refined on F^2 by full-matrix least-squares methods using the SHELXL-2017 program in the WinGX package [15-17].

2.3 Thermal Measurements

DSC and TG-DTA measurements were carried out in the temperature ranges of 98–333 K and 300–1600 K, respectively, using DSC7020 and TG-DTA7300 systems from Seiko Instruments Inc. Aluminium (for DSC) and platinum (for TG-DTA) open pans with no pan cover were used as measuring vessels and reference pans. Fine powder samples, prepared by grinding several pieces of crystals, were used for the measurements.

3. RESULTS AND DISCUSSION

3.1 Crystal Structure

The crystal structure of the grown crystals was determined at room temperature using the single-crystal X-ray diffraction method. The lattice parameters calculated from all observed reflections showed that the crystal belongs to an orthorhombic system. The intensity statistics and systematic extinctions of the X-ray reflections revealed that the structure has a centric space group *Pbca*. Thus, the crystal structure was determined to be orthorhombic *Pbca* with cell parameters a = 18.0136(7) Å, b = 13.9487(4) Å, and c = 6.4838(2) Å. The atomic coordinates and thermal parameters of all atoms in DL-$PbC_4H_4O_6{\cdot}2H_2O$, including hydrogen atoms, were refined with orthorhombic *Pbca*, and a final *R*-factor of 3.75 % was obtained for 2941 unique observed reflections.

The relevant crystal data, and a summary of the intensity data collection and structure refinement parameters are given in Table 1. Fig. 2 shows a projection of the DL-$PbC_4H_4O_6{\cdot}2H_2O$ crystal structure along the *c*-axis. The positional parameters in fractions of the unit cell and the thermal parameters are listed in Table 2. Selected bond lengths and angles are given in Table 3, and the hydrogen-bond geometry is presented in Table 4.

The observed lattice constants of DL-$PbC_4H_4O_6{\cdot}2H_2O$ differ from those previously reported for L-$PbC_4H_4O_6$, and the volume of the unit cell (1629.16(9) $Å^3$) is almost three times larger than that (589.31(3) $Å^3$) of L-$PbC_4H_4O_6$ [13]. Moreover, the calculated density of 3.191 Mg m^{-3} is lower than that of L-$PbC_4H_4O_6$, which is 4.004 Mg m^{-3}. Sixteen water molecules, which were taken from the solution used for crystallisation, are present in the unit cell of the observed structure, while there are no corresponding water molecules in the L-$PbC_4H_4O_6$ crystal. This difference is likely related to the difference in the density.

The obtained structure of DL-$PbC_4H_4O_6{\cdot}2H_2O$ consists of PbO_8 polyhedra, $C_4H_4O_6$ molecules, and two independent H_2O molecules, and there are O–H···O and C–H···O hydrogen bonds between adjacent $C_4H_4O_6$ or H_2O molecules. Each Pb atom in the unit cell is surrounded by eight O atoms forming the PbO_8 polyhedron, as listed in Table 3. The lengths of the Pb–O bonds are in the range of 2.390(4)–3.071(6) Å, and the average Pb–O distance in the polyhedron is 2.666 Å. Then, the volume of the polyhedron is slightly smaller than that (the average one of 2.695 Å) in L-$PbC_4H_4O_6$ [13]. The lengths of single and double O–C bonds in organic molecules are respectively around 1.43 and 1.22 Å, and the length of single C–C bonds is around 1.54 Å. Therefore, the O–C bonds (with lengths of 1.426(6) and 1.416(7) Å) of hydroxyl groups in the $C_4H_4O_6$ molecule have single-bond character, and the remaining four bonds (in the range of 1.226(6)–1.273(6) Å) have double-bond character. Moreover, the three C–C bonds (in the range of 1.521(7)–1.531(7) Å) have single-bond character. The characteristics of these bond types are very similar to those of L-$PbC_4H_4O_6$, DL-$BaC_4H_4O_6{\cdot}H_2O$, and other tartrate salts [4,5,13,14]. The angle between the two least-squares planes of atoms, [O(1)O(2)O(3)C(1)C(2) and O(4)O(5)O(6)C(3)C(4)], in the $C_4H_4O_6$ molecule was calculated to be 80.2(2)°, which is nearly a right angle. The angle in the L-$PbC_4H_4O_6$ crystal was calculated using the published positional parameters to be 60.6°. The obtained angle of DL-$PbC_4H_4O_6{\cdot}2H_2O$ is larger than those of L-$PbC_4H_4O_6$ and other tartrate salts [4,5,13,14].

The O–H···O and C–H···O hydrogen bonds connect adjacent $C_4H_4O_6$ or H_2O molecules. The zig-zag hydrogen-bonded chains along the *a*- and *b*-axes, as shown in Fig. 2, are constructed by the O–H···O bonds. The lengths of the O–H···O bonds are in the range of 2.657(6)–3.125(8) Å, while those of the C–H···O bonds are in the range of 3.506(7)–4.281(7) Å, as shown in Table 4. The O–H···O bonds are typically shorter than the C–H···O bonds. The magnitude of bonding strength is mainly reflected in the bond length. Thus, the bonding strength of the O–H···O bonds is stronger than that of the C–H···O bonds.

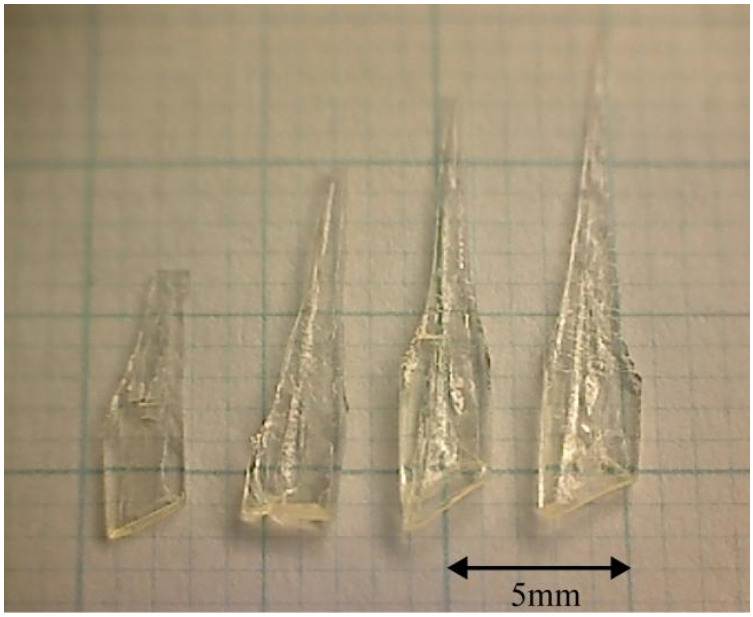

Fig. 1. Photograph of DL-$PbC_4H_4O_6 \cdot 2H_2O$ crystals grown by the gel method

Table 1. Crystal data, intensity data collection, and structure refinement for DL-$PbC_4H_4O_6 \cdot 2H_2O$

Compound, M_r	$PbO_8C_4H_8$, 391.30
Crystal shape, color	Plate, colorless
Measurement temperature	299 K
Crystal system, space group	Orthorhombic, *Pbca*
Lattice constants	a = 18.0136(7) Å, b = 13.9487(4) Å
	c = 6.4838(2) Å
V, Z	1629.16(9) $Å^3$, 8
D(cal.), μ(Mo K_α), F(000)	3.191 Mg m^{-3}, 20.73 mm^{-1}, 1424
Crystal size	0.14×0.18×0.20 mm^3
θ range for data collection	2.69–34.99°
Index ranges	$-28 \le h \le 28$, $-22 \le k \le 22$, $-10 \le l \le 10$
Reflections collected, unique	39554, 3596 [R(int) = 0.0674]
Completeness to θ_{max}	99.9 %
Absorption correction type	Numerical
Transmission factor T_{min}–T_{max}	0.0330–0.1346
Date, parameter	2941 [$I > 3\sigma(I)$], 151
Final R indices	R_1 = 0.0375, wR_2 = 0.0693
R indices (all data)	R_1 = 0.0546, wR_2 = 0.0765
Weighting scheme	$w=1/[\sigma^2(F_o^2)+(0.0196P)^2+6.687P]$
	$P = (F_o^2+2F_c^2)/3$
Goodness-of-fit on F^2	1.296
Extinction coefficient	0.00129(7)
Largest diff. peak and hole	2.138 and -2.605 e $Å^{-3}$

Table 2. Atomic coordinates and thermal parameters (×10^4 Å^2) for DL-$PbC_4H_4O_6 \cdot 2H_2O$ at room temperature, with standard deviations in brackets. The anisotropic thermal parameters are defined as exp[$-2\pi^2(U_{11}a^{*2}h^2+U_{22}b^{*2}k^2+U_{33}c^{*2}l^2+2U_{23}b^*c^*kl+2U_{13}a^*c^*hl+2U_{12}a^*b^*hk)$]. The isotropic thermal parameters (Å^2) for H atoms are listed under U_{11}

Atom	*X*	*Y*	*Z*	U_{11}	U_{22}	U_{33}	U_{23}	U_{13}	U_{12}
Pb	0.39327(2)	0.06299(2)	0.54396(3)	176.8(9)	280.5(10)	206.9(10)	-8.1(7)	2.2(7)	3.3(7)
C(1)	0.1996(3)	0.1045(4)	0.3234(8)	195(21)	259(23)	197(23)	47(19)	28(17)	36(18)
C(2)	0.1246(3)	0.1152(4)	0.4298(8)	163(19)	241(21)	189(23)	21(18)	25(16)	35(16)
C(3)	0.1333(3)	0.1087(4)	0.6627(8)	172(19)	231(21)	181(23)	-13(18)	13(17)	-21(17)
C(4)	0.0582(3)	0.1268(3)	0.7663(8)	204(21)	233(21)	183(22)	-51(18)	-12(18)	-6(17)
O(1)	0.2530(2)	0.1496(3)	0.3971(7)	238(19)	394(22)	424(25)	-105(21)	72(18)	-108(16)
O(2)	0.2043(2)	0.0502(3)	0.1676(6)	185(16)	459(24)	261(20)	-138(18)	26(15)	24(16)
O(3)	0.0739(2)	0.0442(3)	0.3575(6)	158(16)	368(22)	245(19)	-79(16)	0(15)	6(14)
O(4)	0.1583(2)	0.0168(3)	0.7235(7)	173(17)	351(21)	263(20)	79(16)	64(15)	81(15)
O(5)	0.0378(2)	0.0688(3)	0.9068(6)	184(16)	323(19)	289(19)	43(16)	72(15)	23(15)
O(6)	0.0225(3)	0.1968(3)	0.7096(7)	428(24)	394(23)	352(23)	19(20)	83(20)	209(20)
O(7)	0.4450(3)	0.1462(3)	0.2041(7)	290(21)	329(21)	287(22)	65(18)	-30(18)	-73(17)
O(8)	0.3224(4)	0.3351(5)	0.4148(10)	453(30)	412(30)	436(31)	-71(23)	65(26)	-127(25)
H(1)	0.108(3)	0.182(5)	0.383(11)	0.03(2)					
H(2)	0.168(3)	0.163(4)	0.709(9)	0.03(2)					
H(3)	0.035(5)	0.065(6)	0.362(14)	0.06(3)					
H(4)	0.192(5)	0.018(6)	0.705(14)	0.06(3)					
H(5)	0.420(5)	0.157(6)	0.128(14)	0.05(3)					
H(6)	0.473(5)	0.203(6)	0.213(13)	0.05(2)					
H(7)	0.296(5)	0.357(7)	0.479(15)	0.10(3)					
H(8)	0.304(5)	0.295(7)	0.397(15)	0.06(3)					

Table 3. Selected interatomic distances (in Å) and angles (in degrees)

Pb–O(1)	2.958(5)	Pb–O(2)^{1}	2.496(4)
Pb–O(3)^{1}	2.592(4)	Pb–O(4)^{2}	2.534(4)
Pb–O(5)^{2}	2.390(4)	Pb–O(5)^{3}	2.624(4)
Pb–O(7)	2.659(4)	Pb–O(8)^{4}	3.071(6)
O(1)–C(1)	1.245(6)	O(2)–C(1)	1.265(6)
O(3)–C(2)	1.426(6)	O(4)–C(3)	1.416(7)
O(5)–C(4)	1.273(6)	O(6)–C(4)	1.226(6)
C(1)–C(2)	1.525(7)	C(2)–C(3)	1.521(7)
C(3)–C(4)	1.531(7)		
O(1)–C(1)–O(2)	123.8(5)	O(1)–C(1)–C(2)	117.5(5)
O(2)–C(1)–C(2)	118.7(5)	O(3)–C(2)–C(1)	110.5(4)
O(3)–C(2)–C(3)	110.6(4)	O(4)–C(3)–C(2)	111.3(4)
O(4)–C(3)–C(4)	108.0(4)	O(5)–C(4)–O(6)	124.8(5)
O(5)–C(4)–C(3)	117.7(4)	O(6)–C(4)–C(3)	117.6(5)
C(1)–C(2) –C(3)	110.6(4)	C(2)–C(3)–C(4)	109.6(4)

(Symmetry codes: (1) -x+1/2, -y, z+1/2; (2) -x+1/2, -y, z-1/2; (3) x+1/2, y, -z+3/2; (4) x, -y+1/2, z+1/2)

Table 4. Hydrogen bond distances (in Å) and angles (in degrees)

D–H···A	D–H	H···A	D···A	<D–H···A
O(3)–H(3)···O(7)^{1}	0.77(9)	2.02(9)	2.753(6)	161(9)
O(4)–H(4)···O(2)^{2}	0.61(9)	2.11(9)	2.670(6)	151(11)
O(7)–H(5)···O(8)^{3}	0.69(9)	2.23(9)	2.909(8)	167(10)
O(7)–H(6)···O(6)^{4}	0.94(9)	1.73(9)	2.657(6)	167(8)
O(8)–H(7)···O(2)^{5}	0.71(9)	2.42(9)	3.125(8)	173(11)
O(8)–H(8)···O(1)	0.66(10)	2.22(10)	2.877(7)	169(11)
C(2)–H(1)···O(6)^{3}	1.03(7)	2.54(7)	3.506(7)	156(5)
C(3)–H(2)···O(8)^{5}	1.03(6)	3.09(6)	3.859(8)	133(4)
C(3)–H(2)···O(1)^{5}		3.27(6)	4.281(7)	171(5)

(Symmetry codes: (1) x-1/2, y, -z+1/2; (2) -x+1/2, -y, z+1/2; (3) x, -y+1/2, z-1/2; (4) x+1/2, -y+1/2, -z+1; (5) x, -y+1/2, z+1/2)

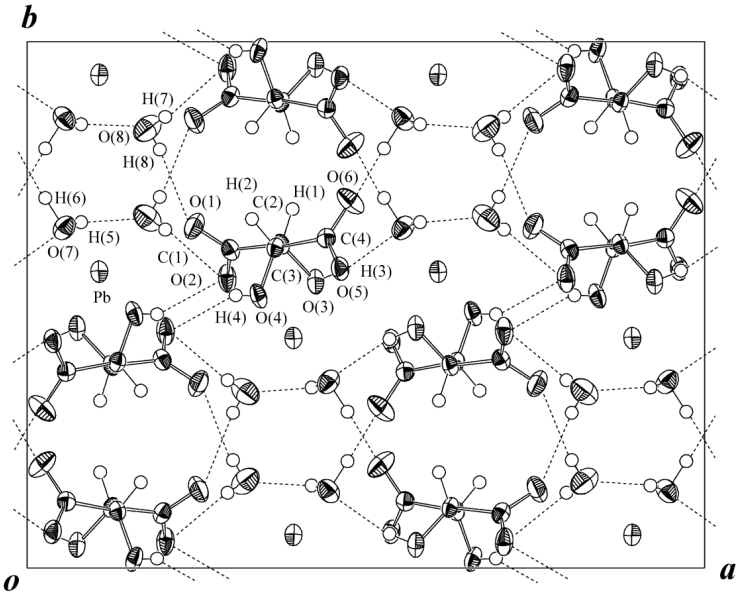

Fig. 2. Projection of the crystal structure of DL-PbC$_4$H$_4$O$_6$·2H$_2$O along the *c*-axis, with 60% probability-displacement thermal ellipsoids. The solid and dashed short lines indicate O–H···O hydrogen bonds, as shown in Table 4

A monoclinic structure (space group $P2_1/c$, Z=8), with cell parameters a = 9.3766(2) Å, b = 7.8919(1) Å, c = 19.0557(4) Å, and β = 91.188(1)°, was detected in only one of many samples. Refinement of the structure including Pb site occupancies gave a final R-factor of 3.22 % (R_w = 5.87 %) for 5374 unique reflections having $I > 2\sigma(I)$. The occupancies of Pb and Si (taken from silica gel) atoms at each of two Pb sites were obtained to be 0.59 and 0.41, respectively. Then, the chemical formula was determined to be $Pb_{0.59}Si_{0.41}C_4H_4O_6{\cdot}H_{1.18}O$ using charge compensation. The $P2_1/c$ structure, including relative placements of water molecules, was very close to that of DL-$BaC_4H_4O_6{\cdot}H_2O$ previously reported, except for differences between the Pb(Si) and Ba cations [14]. Moreover, the average electric charge 54e (= 82e × 0.59 + 14e × 0.41) [C] and atomic weight 133.8 (= 207.2 × 0.59 + 28.1 × 0.41) [g mol^{-1}] on the Pb sites were very close to those (56e [C] and 137.3 [g mol^{-1}], respectively) of the Ba atom. We concluded that the appearance of the $P2_1/c$ structure in the DL-$PbC_4H_4O_6{\cdot}2H_2O$ crystal is caused by the decreases in electric charge and atomic weight at the Pb sites by the substitution of Pb^{2+} with Si^{4+} ions in silica gel.

3.2 Thermal Analysis

Fig. 3 shows the DTA, TG, and differential TG (DTG) curves of the DL-$PbC_4H_4O_6{\cdot}2H_2O$ crystal in the temperature range of 300–1600 K. The sample weight (powder) used for the measurements was 4.51 mg, and the heating rate was 10 K min^{-1} under a nitrogen gas flow of 300 ml min^{-1}. The DTA curve exhibits six endothermic peaks at 367.6, 481.2, 572.9, 1054.4, 1153.3, and 1196.4 K, including small peaks. Moreover, six peaks at 366.7, 491.3, 571.9, 1135.8, 1183.4, and 1501.2 K, including small peaks, are also observed in the DTG curve. These DTA peaks correspond relatively closely to the respective DTG peaks. The DTG curve, which is the first derivative of TG curve, reveals the temperature dependence of the rate of weight loss. Thus, the DTA peaks are associated with the maximum rate of weight loss in the TG curve due to thermal decomposition of the sample. DSC measurements on the powder sample of DL-$PbC_4H_4O_6{\cdot}2H_2O$ were performed in the temperature range from 98 to 333 K at a heating rate of 5 K min^{-1}. No obvious endothermic or exothermic peaks were observed in the temperature range of the DSC curve. In general, it is believed that a clear peak in DSC (or DTA) curve is attributed to the change in exchange energy at a phase transition. Thus, the obtained results indicate that there is no phase transition in the temperature range of 98–367 K for the DL-$PbC_4H_4O_6{\cdot}2H_2O$ crystal.

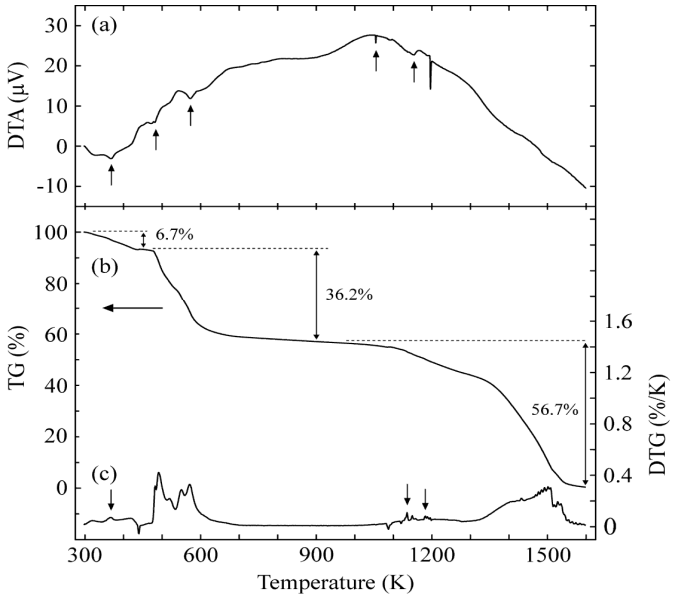

Fig. 3. TG, DTG, and DTA thermograms for DL-$PbC_4H_4O_6{\cdot}2H_2O$ crystal on heating. The sample weight (powder) was 4.51 mg, and the heating rate was 10 K min^{-1} under a dry N_2 flux of 300 ml min^{-1}

The observed TG curve, which describes the temperature-dependent weight loss of the DL-$PbC_4H_4O_6{\cdot}2H_2O$ crystal, slightly differs from those of other tartaric salts previously reported [4,5,14]. Two large weight losses in the TG curve are seen at around 500 K and 1400 K. The weight losses in the temperature ranges of 300–450, 450–900, and 900–1600 K were observed to be 6.7, 36.2, and 56.7%, respectively, as described in Fig. 3. The weight losses in the TG curve are thought to be caused by the evolution of gases from the sample, similar to previous reports [4,5,14]. Unfortunately, since the thermal loss processes in the TG curve at around 500 K are observed over a narrow temperature range, detailed information of the processes cannot be obtained. We assume that two crystallographically independent H_2O molecules in the crystal evaporate with increasing temperature. The theoretical loss rate due to the evaporation of $2H_2O$ is calculated to be 9.2 % (= 36.0 / 391.3). This calculated value is slightly larger than the experimental value (6.7 %) in the range of 300–450 K. This indicates that complete evaporation of all water molecules does not occur in the range of 300–450 K, and specifically, one quarter of water molecules (four water molecules in the unit cell) remain in the crystal. Moreover, we assume that the evolution of gases ($2H_2$, 3CO, and CO_2) from the $C_4H_4O_6$ molecule and the generation of PbO with the Pb atom and an O atom isolated from the molecule occur at temperatures above 450 K. The theoretical loss rate due to the evaporation of gases ($2H_2$, 3CO, and CO_2) from $C_4H_4O_5$ is calculated to be 33.8 % (= 132.1 / 391.3), which is slightly smaller than the experimental value (36.2 %) in the range of 450–900 K. However, the total theoretical loss of 43.0 % (= 9.2 + 33.8 %) calculated from the evaporation of $2H_2O$ and $C_4H_4O_5$ is very close to the experimental value of 42.9 % (= 6.7 + 36.2 %) in the range of 300–900 K. Thus, the weight losses in this temperature range are considered to be caused by the evolution of gases from $2H_2O$ and $C_4H_4O_5$. We assume that the loss around 1400 K is produced by the evolution of Pb and $(1/2)O_2$ gases due to thermal decomposition of PbO. The theoretical loss rate due to the evaporation of PbO is calculated to be 57.0 % (= 223.2 / 391.3). This value is very close to the experimental value of 56.7 % in the range of 900–1600 K. The total experimental weight loss in the range of 300–1600 K is 99.6 % (= 6.7 + 36.2 + 56.7 %) and the remaining mass of 0.4 % is retained in the vessel. After heating up to 1600 K in the TG-DTA measurements, we found that a very small transparent material was present in the vessel. The remaining material probably contains silicon compounds that consist of Si atoms incorporated into the crystals during the crystal growth, as mentioned in the results for the $P2_1/c$ structural analysis.

4. SUMMARY

Single crystals of DL-$PbC_4H_4O_6{\cdot}2H_2O$ were grown in silica gel medium at 308 K by the diffusion method. The thermal properties and crystal structure on the single crystals were studied by means of DSC, TG-DTA, and X-ray diffraction. The room-temperature crystal structure, including the positional and thermal parameters of all hydrogen atoms, was determined to be orthorhombic with space group *Pbca*. The structure consists of PbO_8 polyhedra, $C_4H_4O_6$ molecules, and two independent H_2O molecules, and has O–H···O and C–H···O hydrogen bonds between adjacent $C_4H_4O_6$ or H_2O molecules. Moreover, there are zig-zag hydrogen-bonded chains along the *a*- and *b*-axes linked by the O–H···O bonds. The monoclinic $P2_1/c$ structure induced by the substitution of Pb^{2+} with Si^{4+} ions in silica gel was confirmed to exist in the DL-$PbC_4H_4O_6{\cdot}2H_2O$ crystal. The appearance of the $P2_1/c$ structure was concluded to be caused by the decreases in electric charge and atomic weight at the Pb sites. No phase transition was observed in the temperature range of 98–367 K, and the weight losses due to thermal decomposition of DL-$PbC_4H_4O_6{\cdot}2H_2O$ were found to occur in the temperature range of 300–1600 K. The weight losses in the temperature ranges of 300–900 K and 900–1600 K were caused by the evolution of gases from $2H_2O$ and $C_4H_4O_5$, and the evaporation of PbO, respectively.

COMPETING INTERESTS

Authors have declared that no competing interests exist.

REFERENCES

1. Desai CC, Patel AH. Crystal data for ferroelectric $RbHC_4H_4O_6$ and $NH_4HC_4H_4O_6$ crystals. J Mater Sci Lett. 1988;7(4):371–373.
Available:https://doi.org/10.1007/BF01730747
2. Bail AL, Bazin D, Daudon M, Brochot A, Robbez-Massond V, Maisonneuve V. Racemic calcium tartrate tetrahydrate

[form (II)] in rat urinary stones. Acta Crystallogr. 2009;B65(3):350–354.
DOI: 10.1107/S0108768109013688

3. Labutina ML, Marychev MO, Portnov VN, Somov NV, Chuprunov EV. Second-order nonlinear susceptibilities of the crystals of some metal tartrates. Crystallogr Rep. 2011;56(1):72–74.
DOI: 10.1134/S1063774510061082
4. Fukami T, Tahara S, Yasuda C, Nakasone K. Crystal structure and thermal properties of $SrC_4H_4O_6{\cdot}4H_2O$ single crystals. Int Res J Pure Appl Chem. 2016;11(1):23674 1–10.
DOI: 10.9734/IRJPAC/2016/23674
5. Fukami T, Hiyajyo S, Tahara S, Yasuda C. Thermal properties and crystal structure of $BaC_4H_4O_6$ single crystals. Inter J Chem. 2017;9(1):30–37.
DOI: 10.5539/ijc.v9n1p30
6. Fukami T, Tahara S, Yasuda C, Nakasone K. Structural refinements and thermal properties of L(+)-tartaric, D(–)-tartaric, and monohydrate racemic tartaric acid. Inter J Chem. 2016;8(2):9–21.
DOI: 10.5539/ijc.v8n2p9
7. Bootsma GA, Schoone JC. Crystal structures of mesotartaric acid. Acta Crystallogr. 1967;*22*(4):522–532.
DOI: 10.1107/S0365110X67001070
8. Song QB, Teng MY, Dong Y, Ma CA, Sun J. (2S,3S)-2,3-Dihydroxy-succinic acid monohydrate. Acta Crystallogr. 2006; E62(8):o3378–o3379.
DOI: 10.1107/S1600536806021738
9. Abdel-Kader MM, El-Kabbany F, Taha S, Abosehly AM, Tahoon KK, El-Sharkawy AA. Thermal and electrical properties of ammonium tartrate. J Phys Chem Solids. 1991;52(5):655-658.
DOI: 10.1016/0022-3697(91)90163-T
10. Torres ME, Peraza J, Yanes AC, López T, Stockel J, López DM, Solans X, Bocanegra E, Silgo GG. Electrical conductivity of doped and undoped calcium tartrate. J Phys Chem Solids. 2002;63(4):695–698.
DOI: 10.1016/S0022-3697(01)00216-5
11. Firdous A, Quasim I, Ahmad MM, Kotru PN. Dielectric and thermal studies on gel grown strontium tartrate pentahydrate crystals. Bull Mater Sci. 2010;33(4):377–382.
DOI: 10.1007/s12034-010-0057-1
12. De Ridder DJA, Goubitz K, Sonneveld EJ, Molleman W, Schenk H. Lead tartrate from X-ray powder diffraction data. Acta Crystallogr. 2002;C58(12):m596–m598.
DOI: 10.1107/S0108270102019637
13. Weil M. Crystal structure of lead(II) tartrate: A redetermination. Acta Crystallogr. 2015; E71(1):82–84.
DOI: 10.1107/S2056989014027376
14. Fukami T, Hiyajyo S, Tahara S. Structural and thermal studies on racemic $BaC_4H_4O_6{\cdot}H_2O$. Chem Sci Inter J. 2017; 20(3):36656 1-10.
DOI: 10.9734/CSJI/2017/36656
15. Burla MC, Caliandro R, Camalli M, Carrozzini B, Cascarano GL, Giacovazzo C, Mallamo M, Mazzone A, Polidori G, Spagna R. SIR2011: A new package for crystal structure determination and refinement. J Appl Crystallogr. 2012;45(2): 357–361.
DOI: 10.1107/S0021889812001124
16. Sheldrick GM. Crystal structure refinement with SHELXL. Acta Crystallogr. 2015;C71(1):3–8.
DOI: 10.1107/S2053229614024218
17. Farrugia LJ. WinGX and ORTEP for Windows: an update. J Appl Crystallogr. 2012;45(4):849–854.
DOI: 10.1107/S0021889812029111

Peer-review history:
The peer review history for this paper can be accessed here:
http://www.sciencedomain.org/review-history/27566